Estimating the hydraulic profiles in a cross-section under one-dimensional steady-flow dynamics by employing the entropy maximization principle: I. Theoretical concepts

3 authors:

Panayiotis Dimitriadis
National Technical University of Athens

Antonis D. Koussis
National Observatory of Athens

Demetris Koutsoyiannis
National Technical University of Athens

Estimating the hydraulic profiles in a cross-section under one-dimensional steady-flow dynamics by employing the entropy maximization principle: I. Theoretical concepts

Panayiotis Dimitriadis*[1,2], Evangelos Rozos[1], Katerina Mazi[1], Antonis D. Koussis[1], and Demetris Koutsoyiannis[2]

[1]Institute for Environmental Research and Sustainable Development, National Observatory of Athens

[2]Department of Water Resources and Environmental Engineering, National Technical University of Athens

*corresponding author; email: pandim@itia.ntua.gr

Abstract

One of the key issues in hydrology is the estimation of streamflow, bathymetry, and water-pressure in rivers through non-invasive practices. This study investigates the streamwise velocity, pressure and water-depth spatial-deterministic profiles in a cross-section under incompressible one-dimensional steady-flow dynamics. We implement a probabilistic-deterministic framework where the profiles can be determined by treating the above variables as random. We focus on the absolute spatial derivative of the three variables and show how it can be linked to their actual profiles. In particular, the spatial derivative can be estimated from the probability distribution function of each variable, on the assumption of positively or negatively monotonic behaviour with respect to the location variable, and on the principle of entropy maximization with typical hydraulic conditions and statistical constraints (i.e. conservation of mass, linear momentum rate, and energy rate), and under a uniform distribution for the location variable in the cross-section. The resulting distributions are the exponential or Gaussian one for the water-depth and pressure and a three-parameter one for the velocity, which often can be well approximated by other flexible and easily handled distributions. Through theoretical reasoning, we show that the above configuration exhibits several advantages as compared to established analyses. Finally, we discuss how the above framework can be used for streamflow, bathymetry and pressure estimation in rivers, with illustrative applications in the companion work of Dimitriadis et al. (2019b).

Keywords: entropy-maximization; 1d steady-flow dynamics; velocity profile; pressure profile; water-depth profile; sampling strategy

1. Introduction

The mathematical branch of stochastics has been widely developed to model the so-called random, i.e., unpredictable, fluctuations recorded in non-linear geophysical systems and to help develop a unified description of natural phenomena, while expelling dichotomies like random *vs*. deterministic. Particularly, it seems that rather both randomness and predictability coexist and are intrinsic to natural systems that can be deterministic and random at the same time, depending on the prediction horizon and the time scale (Koutsoyiannis, 2010). In other words, the line distinguishing determinism (i.e., predictability) and randomness (i.e., unpredictability) is related to the scale of the time-window within which the future state deviates from a deterministic prediction by an error threshold. Therefore, by applying a stochastic process we enable the generation of an ensemble of realizations, while observation of the given natural system can only produce a single observed time series or multiple ones in repeatable experiments (Dimitriadis et al., 2016a).

In this work, we focus on the intrinsic uncertainty and deterministic conditions of the steady streamflow process and we investigate how it can be quantified through the time-averaged surface velocity, pressure and water-depth in a natural open-channel cross-section. For this, we adopt the concept and methodology introduced by Chiu (1987) of applying a maximum-entropy-based stochastic framework for discharge estimation in natural open channels, and show specifically how it can be linked to deterministic velocity, pressure and water-depth distributions. This framework has been applied to several flow conditions such as open-channel flow (Chiu, 1988; 1989), circular pipe flow (Chiu et al., 1993; Chiu and Hsu, 2005; Yoon et al., 2012; Singh, 2014; Jiang et al., 2016; Choo et al., 2017; Kazemian et al., 2018), unsteady tidal flow (Chen and Chui, 2002; Chen et al., 2012; Bechle and Wu, 2014); with additional than the mean constraints (Chiu, 1989; Barbe et al., 1991; Singh, 2014; Kumbhakar, et al., 2019a); with alternate entropy measures (Cui and Singh, 2013; 2014; Sing and Luo, 2014; Kumbhakar and Ghoshal, 2016; Khozani and Bonakdari, 2018; Kumbhakar et al., 2019b,c); for different geometries of the open-channel cross-section such as with wide or narrow two-dimensional rectangular shapes (Chiu, 1988; Araujo and Chaudhry, 1998; Marini et al., 2011; 2017; Singh et al., 2013; Fontana et al., 2013; Singh, 2014; Mirauda et al., 2018) or irregular shapes (Chiu and Murray, 1992; Moramarco et al., 2004; Singh, 2014); accounting for channel roughness (Chiu, 1991; Greco et al., 2014; Singh, 2014; Greco, 2015; Greco and Mirauda, 2015; Greco and Moramarco, 2015; Wibowo, 2015); for the design of irrigation ditches (Greco, 2016), for bathymetry estimation (Moramarco et al., 2013; 2019; Farina et al., 2015); for the structure of furrow geometry (Sighn, 2012), open-channel with submerged aquatic plants (Chen and Kao, 2011); for the derivation of the streamwise isovelocity contours (Chiu, 1989; Maghrebi and Rahimpour, 2005; 2006); for sediment flow and bed-load thickness (Chiu, 1987; Kumbhakar et al., 2017a,b, 2018; Zhu and Yu, 2019); for the scour depth (Pizarro et al., 2017); for the shear stress (Chiu, 1987; Singh, 2014; Sheikh and Bonakdari, 2015; Kazemian et al., 2019a); for the piezometric head in groundwater flow (Barbe et al., 1994); abundant applications in other hydrological and hydraulic fields can be found in Singh (2014).

The standard practice for estimating the discharge at a cross-section of a channel is to point-sample the velocity field, assuming steady-state hydraulics and stable channel geometry measurable with good accuracy over short times. Such a practice is tedious, often dangerous, and even infeasible under high flows; the non-uniform longitudinal velocity is sampled at multiple locations in a cross-section, commonly at 20%, ~60% and 80% of the depth on a number of verticals. The selection of those locations is semi-empirical; it is guided by the idealised deterministic model of the Prandtl-von Kàrman logarithmic velocity profile (see also application in sect. 2.3 and in the companion work of Dimitriadis et al., 2019b, sect. 3.1.1) of normal, turbulent flow in an infinitely wide channel. The traditional framework allows for the implicit determination of the streamflow by a few samples such as the velocities at boundaries and surface, which can be nowadays measured with non-invasive methods, and the location and magnitude of the maximum velocity within the cross-section when the dip-phenomenon occurs (Chiu, 1988; Xia, 1997; Chen and Chiu, 2004; Moramarco et al., 2004; Chiu et al., 2005; Papadimitrakis and Orphanos, 2009; Singh, 2014; Chiu and Hsu, 2016; Moramarco et al., 2017). The other model parameters are assumed constant in a fixed cross-section in the sense that they mainly vary due to hydraulic conditions and due to several hydraulic properties of the cross-section that may be assumed unchangeable for a relatively long time-period such as roughness and geometry of the cross-section. These parameters may be estimated theoretically only once, as for example when the river can be accessible for velocity point-sampling throughout the whole cross-section (Chiu and Said, 1995; Farina et al., 2014), and with relatively small errors on the streamfllow estimation of the order of 10% (Fulton and Ostrowski, 2008; Chen et al., 2013; see also discussion in Dimitriadis et al., 2019b, sect. 3.4).

The revisited probabilistic-deterministic framework focuses on the absolute values of the spatial derivatives with respect to location of the velocity, pressure water-depth, which, as shown in the next sections, exhibits several advantages as compared to the traditional analysis of the regular spatial variables. In section 2, we present some statistical tools and probabilistic analyses related to the so-called change-of-variable technique. In section 3, we show how the previous technique can be linked to the principle of maximum entropy, and we derive general deterministic profiles for the velocity, pressure and water-depth emerging from the one-dimensional hydraulic conservation of mass, linear momentum rate and energy rate in a cross-section. Finally, in section 4, we discuss on the limitations and strengths of the proposed framework. We note that several applications on open-channel flow with small and large width-to-depth ratios, irregular geometries, spillways, and on pipe flow of symmetrical cross-sections, can be found in the companion work of Dimitriadis et al. (2019b).

2. Methodology

In this section, we present the probabilistic-deterministic methodology for applications in hydraulics based on Chiu's (1988) original methodology, but also introduce some new concepts with focus on the probability distribution function of the velocity (in short *velocity distribution*), pressure (in short *pressure distribution*) and water-depth (in short *depth distribution*), and how they can be linked to the deterministic functions of the velocity, pressure and water-depth with respect to location (in short *velocity profile, pressure profile*, and *depth profile*) through uniform sampling of the location on a cross-section (in short *location distribution* or *sampling distribution*).

2.1. Concepts of methodology and definitions

We wish to derive an expression of the time-averaged velocity, pressure and water-depth as a function of the geometry of a natural cross-section in incompressible steady-state flow conditions. All models are obviously connected to the Reynolds shear stress model, which is a key assumption in computational fluid dynamics (e.g., Schmitt, 2007). Therefore, the examined task could be done deterministically by employing the Navier-Stokes equations (i.e., conservation of mass, momentum, energy etc.) either through analytical reasoning under several assumptions or numerically through computational fluid dynamic schemes. However, this deterministic approach cannot easily handle the intrinsic uncertainty of the natural processes, since we would require almost infinite information to deterministically study the velocity in every water *parcel* (lump) within a river section. Therefore, we could apply a combined deterministic-probabilistic approach that can not only handle as constraints simple deterministic (analytical or empirical) solutions of the Navier-Stokes under reasonable assumptions (e.g., steady-state, uniform-flow, turbulent-regime), but that could also properly handle the uncertain components of the natural process by maximizing the effect of any available information from recorded field data. This approach can be also applied considerably easier as compared to the purely deterministic one, and could be even expanded to take into consideration additional hydraulic flow conditions such as rotationality

(Joseph, 2006), viscosity (Prandtl, 1905), etc. However, such effects can be often neglected in geometries and conditions often met in natural rivers.

The three key variables in fluid mechanics are the vector velocity (measured in m/s), pressure (measured in m; standardized by ρg, with ρ the water density and g the gravity acceleration, both assumed constant), and water-depth (measured in m). Here, we analyse the longitudinal velocity and pressure, as well as the water-depth within a cross-section. Note that we adopt the Dutch convention (Hemelrijk, 1966), where a random variable is underlined to be distinguished from a regular one, which denotes the support values of the random variable, and a hat over a variable denotes an estimation function (or else called estimator). We treat the velocity v in the cross-section as a random process $\underline{u}(t, x, y)$ spatially distributed within the cross-sectional geometry (x, y) as well as temporally evolving in time t. We further assume that the flow in the cross-section is steady and has been time-averaged, and thus, the random process depends only on the geometrical characteristics of the cross-section, i.e.:

$$\underline{v}(x, y) = \frac{\int_0^T \underline{u}(t, x, y)\mathrm{d}t}{T} \tag{1}$$

where T is the averaging time selected such that the mean value has been reached at each spatial location, and $\underline{v}$ is a random process containing all the random variables $\underline{v}(x, y)$. In a similar manner we define the random process of pressure $\underline{p}(x, y)$, and the water-depth $\underline{w}(x, y)$.

A proper way to continue the analysis would be to investigate the stochastic behaviour of the above three processes (i.e., by estimating their marginal and joint statistical measures), derive from there their spatial dependence, and thus, the velocity, pressure and depth stochastic models. However, this method would require many observations for each variable within several cross-sections. Unfortunately, such a large number of observations is hardly available for natural cross-sections or even from laboratory setups. Alternatively, we may assume a white noise dependence structure for the above processes (i.e., no spatial auto- or joint-correlation), and thus, treat the above variables as random with a marginal distribution $F_{\underline{v}}(v) \coloneqq \mathrm{P}(\underline{v} \leq v)$, $F_{\underline{p}}(p) \coloneqq \mathrm{P}\left(\underline{p} \leq p\right)$, and $F_{\underline{w}}(w) \coloneqq \mathrm{P}(\underline{w} \leq w)$, respectively. In this manner, the realizations of each variable can be randomly distributed within a cross-section. For example, Chiu (1988) proposed the velocity to be uniformly distributed on the isovel lines (i.e., lines within the cross-section, where velocity has unique expected value) that are considered fixed for typical hydraulic conditions. However, since all processes have evidently a structure within the cross-section, Chiu (1988) proposed to represent this by introducing a deterministic function that rearranges the randomly distributed variables. An obvious limitation of this methodology is that after employing the deterministic function the spatial (auto and cross) dependence of all the initially defined random variables $\underline{v}(x, y)$, $\underline{p}(x, y)$ and $\underline{w}(x, y)$ would be again zero (rare case in natural phenomena), and the statistical properties of each point velocity and pressure within the cross-section could be explicitly estimated by the deterministic function and the marginal values (resembling a non-stationary process). Nevertheless, this approach has been proven to be a powerful tool for describing the velocity profile, and so, here, we explore and further advance this theoretical concept as an approximation to the task.

The aforementioned deterministic continuous functions are defined as $\underline{v} = g(\underline{s})$, $\underline{p} = \psi(\underline{s})$, and $\underline{w} = \omega(\underline{s})$, where $s = G(x, \mathrm{y})$ is a function of the area A, with the axis origin arbitrarily set (e.g., if the axis is set at the lowest point of the cross-section, y will denote the water-depth measured from the channel bottom, and x the perpendicular distance). Examples of such deterministic functions are for the water-depth of an oval-type commonly observed in natural cross-sections like the half-circle one of radius R having the maximum hydraulic radius (i.e., maximum wetted area within the smallest available wetted perimeter) with $\omega(x, y) = \sqrt{R^2 - x^2}$ (see an example and sketch in the companion work of Dimitriadis et al., 2019b, sect. 3.2). For the relative pressure, in case of no strong fluid accelerations normal to the flow direction, one may assume a linear hydrostatic profile with $\psi(x, y) = d - y$ (i.e., lines of points with the same vertical distance from the reference level have the same pressure), where d is the maximum vertical distance between the atmospheric pressure level and the reference level (for an example see the companion work of Dimitriadis et al., 2019b, sect. 3.1.3). For the velocity, several models exist depending on the hydraulic conditions of the flow, as for example the one-dimensional Couette model, often met at the sub-viscous area, with the velocity varying linearly with depth, i.e. $g(y) = a\mathrm{y}$, or the von Kàrman logarithmic profile for channels of infinite width with $g(x, y) = \alpha \ln(y/b)$, where α and b are model parameters (for more details see an application in sect. 2.3 and in the companion work of Dimitriadis et al., 2019b, sect. 3.1.1).

We comment that if the shear stress, pressure-gradient or cross-section geometry models are given then one could easily calculate the location of the isolines within the cross-section for each one of the three variables, and vice versa. For example, Chiu (1988) introduced a model for the locations of the iso-velocity lines (or simply called isovels) along a vertical line in the channel based on observations and numerical models (Chiu and Lin, 1983; Chiu and Chiou, 1986), i.e. $\xi(y) = y/(d - h)\mathrm{e}^{1 - y/(d-h)}$, where h is the distance between the water surface and the location of the maximum velocity. Notice that in the latter function one value of ξ corresponds to two depths y due to the non-monotonicity of the function. Chiu (1988) actually introduced this model to tackle the non-monotonicity issue often appearing in hydraulics (e.g., open-channels), which is mainly due to the effects of boundaries on the flow creating secondary currents (else known as dip-phenomenon; Yang et al., 2012).

Along a vertical line the velocity derivative can be expressed as:

$$\frac{\partial g(s)}{\partial s} = \frac{\partial g(\xi)}{\partial \xi} \frac{\partial \xi(y)}{\partial y} \tag{2}$$

In other words, by defining just the location of the isovels within a cross-section, the velocity derivative with respect to depth can be again calculated provided that the derivative of the velocity with respect to isovels, i.e. $\partial g(\xi)/\partial \xi$, is estimated instead of $\partial g(y)/\partial y$, as described above. Chiu (1988) proposed a method to estimate both the velocity derivatives through the entropy maximization principle.

In this work, we follow a similar approach but with focus on the absolute value of the derivative, i.e. for the one-dimensional velocity $|\partial g(y)/\partial y|$, and without the need to acquire any information on the locations of isolines. After the estimation of the absolute value of the derivative one may adopt appropriate assumptions on how the sign of the regular variable varies within the cross-section, and construct the isolines. In fact, for the velocity, two reasonable assumptions for open-channel flows are that the shear stress is continuous in the whole cross-section and that it is mainly caused by the boundary effects from channel bottom and sides, as well as from the water surface. If these assumptions are met then for areas outside the sub-viscous layer, the shear stress along a vertical line should have only one spatial location, where its sign changes and, specifically, at the location of zero value of the second derivative, $\partial^2 g(y)/\partial y^2 = 0$. With this information one may construct the velocity profile without the need of implementing empirical or other theoretical expressions for the isovels (see preliminary results and various applications of the above two assumptions for the shear stress in Dimitriadis et al., 2019a;b).

2.2. Change of random variable through an unknown deterministic function

Based on the above concepts and definitions, it can be easily shown that for a positively monotonic behaviour between the random variables of the velocity and the location (similarly for the pressure and water-depth), we have that (e.g., Benjamin and Cornell, 2014):

$$F_{\underline{s}}(s) = F_{g^{-1}(\underline{v})}(s) = F_{\underline{v}}\big(g(s)\big) \tag{3}$$

where $g^{-1}(v)$ is the single-valued inverse function of $g(s)$. Equivalently, if we start from the distribution of $F_{\underline{v}}(v)$ we have that:

$$F_{\underline{v}}(v) = F_{g(\underline{s})}(v) = F_{\underline{s}}\big(g^{-1}(v)\big) \tag{4}$$

For the general case of negatively or positively monotonic behaviour:

$$\left|\frac{\mathrm{d}g(s)}{\mathrm{d}s}\right| = \frac{f_{\underline{s}}(s)}{f_{\underline{v}}\big(g(s)\big)} \tag{5}$$

and similarly

$$\left|\frac{\mathrm{d}g^{-1}(v)}{\mathrm{d}v}\right| = \frac{f_{\underline{v}}(v)}{f_{\underline{s}}\big(g^{-1}(v)\big)} \tag{6}$$

In Eqs. (5) and (6) $|\mathrm{d}g^{-1}(v)/\mathrm{d}v|_{v=g(s)}$ and $|\mathrm{d}g(s)/\mathrm{d}s|_{s=g^{-1}(v)}$ are the absolute values of the total derivatives of $g^{-1}(v)$ with respect to v estimated on $v = g(s)$, and $g(s)$ with respect to s estimated on $s = g^{-1}(v)$, respectively; and $f_{\underline{s}}(s)$ and $f_{\underline{v}}(v)$ are the probability density distribution functions of $\underline{s}$ and $\underline{v} = g(\underline{s})$, i.e. $f_{\underline{s}}(s) \coloneqq \mathrm{d}F_{\underline{s}}(s)/\mathrm{d}s$ and $f_{\underline{v}}(v) \coloneqq \mathrm{d}F_{\underline{v}}(v)/\mathrm{d}v$, respectively.

Since $F_{\underline{s}}(s)$ can be arbitrarily chosen, estimating $f_{\underline{v}}(v)$ allows for the determination of $v = g(s)$. For example, in case $g(s)$ is monotonic, i.e. $\mathrm{d}g(s)/\mathrm{d}s \geq 0$ or $\mathrm{d}g(s)/\mathrm{d}s \leq 0$, then $g(s)$ can be estimated by solving the nonlinear expression below as a function of the unknown $g(s)$:

$$g(s) = \pm \int_{s_\mathrm{o}}^{s_\mathrm{m}} \frac{f_{\underline{s}}(s)}{f_{\underline{v}}\big(g(s)\big)} \mathrm{d}s \tag{7}$$

where the positive and negative sign holds for a positively and negatively monotonic $g(s)$, respectively, and s_o and s_m are the minimum and maximum limits of s. Note that more than one solution for $g(s)$ may exist.

A useful solution for the inverse function $g^{-1}(v)$ can be derived for a uniform location distribution and a positively monotonic behaviour, i.e.:

$$s = g^{-1}(v) = F_{\underline{v}}(v)\left(g^{-1}(v_\mathrm{m}) - g^{-1}(v_\mathrm{o})\right) + g^{-1}(v_\mathrm{o}) \tag{8}$$

where v_m and v_o are the velocities at locations $s_\mathrm{o} = g^{-1}(v_\mathrm{o})$ and $s_\mathrm{m} = g^{-1}(v_\mathrm{m})$, respectively.

In case of a non-monotonic $g(s)$, the above expression no longer holds and the function $g(s)$ must be divided into n_v branches of monotonic behavior of v, i.e:

$$g(s) = \begin{cases} g_1(s), \text{with sgn}\left(\dfrac{\mathrm{d}g_1(s)}{\mathrm{d}s}\right) = c_1, -\infty < v \leq v_1 \\ \cdots \\ g_n(s), \text{with sgn}\left(\dfrac{\mathrm{d}g_n(s)}{\mathrm{d}s}\right) = c_n, v_{n_v - 1} < v < \infty \end{cases} \tag{9}$$

where c_i are either 1 or -1 for the whole range of $v_{n_v-2} < v \leq v_{n_v-1}$, i is the index for the portions of the function $g(s)$ ranging from 1 to n_v, and v_l are the velocity limits at each portion of $g(s)$ where the derivative of $g(s)$ has a constant sign.

Then, it can be shown that:

$$f_{\underline{s}}(s) = \sum_{i=1}^{n_v} \left|\frac{\mathrm{d}g_i(s)}{\mathrm{d}s}\right| f_{\underline{v}}\big(g_i(s)\big) \tag{10}$$

Since here we are interested in the absolute spatial derivative of $g(s)$ with respect to location, i.e. $|\mathrm{d}g(s)/\mathrm{d}s|$, we may transform the function $g(s)$ to a function $\zeta(s)$ with a monotonic behaviour in the cross-section. In other words, the new function $\zeta(s)$ will be monotonic as compared to the non-monotonic $g(s)$, while both will have equal spatial derivatives with respect to the location, i.e. $|\mathrm{d}\zeta(s)/\mathrm{d}s| = |\mathrm{d}g(s)/\mathrm{d}s|$. If $g(s)$ is known, $\zeta(s)$ can be estimated at every location s_j in the cross-section as:

$$\zeta_i(s_j) = \zeta_i(s_{j-1}) + \left|\frac{\mathrm{d}g_i(s_j)}{\mathrm{d}s}\right| (s_j - s_{j-1}) \tag{11}$$

where j is the index for locations within each portion of $g(s)$ ranging from 1 to n_i, and $\zeta_i(s_0) = \zeta_{i-1}(s_{n_{i-1}})$. Note that we can also get $g(s)$ from $\zeta(s)$ if we know the sings of $g(s)$ derivative for the whole area of the cross-section. The corresponding monotonic functions for the pressure and water-depth are $\psi(s)$ and $\omega(s)$, with $|\mathrm{d}\psi(s)/\mathrm{d}s| = |\mathrm{d}p(s)/\mathrm{d}s|$ and $|\mathrm{d}\omega(s)/\mathrm{d}s| = |\mathrm{d}w(s)/\mathrm{d}s|$, respectively.

Therefore, if the two density functions of the location $F_{\underline{s}}(s)$ and the velocity $F_{\underline{v}}(v)$ are appropriately selected, the positively monotonic deterministic function $\zeta(s)$, which is used to transform one variable to the other, can be estimated, and so does the profile $v = g(s)$.

Finally, we remark that in the presented framework the location variable can be regarded as the way one samples the velocities in a cross-section. For example, if we uniformly sample the velocities that are assumed to be normally distributed along a vertical line, i.e. we take velocity measurements that follow the N(0,1) uniformly distributed over this line (Fig. 1), then $F_{\underline{y}}(y) = (y - y_{\mathrm{o}})/(y_{\mathrm{m}} - y_{\mathrm{o}})$, where the minimum and maximum sampling depths are $y_o = 0$ (channel bottom) and $y_{\mathrm{m}} = d$ (open surface). Equivalently, if the deterministic profile is known then by changing the distribution for sampling, the velocity distribution must be also altered, since the two variables are obviously linked (see next section for an application).

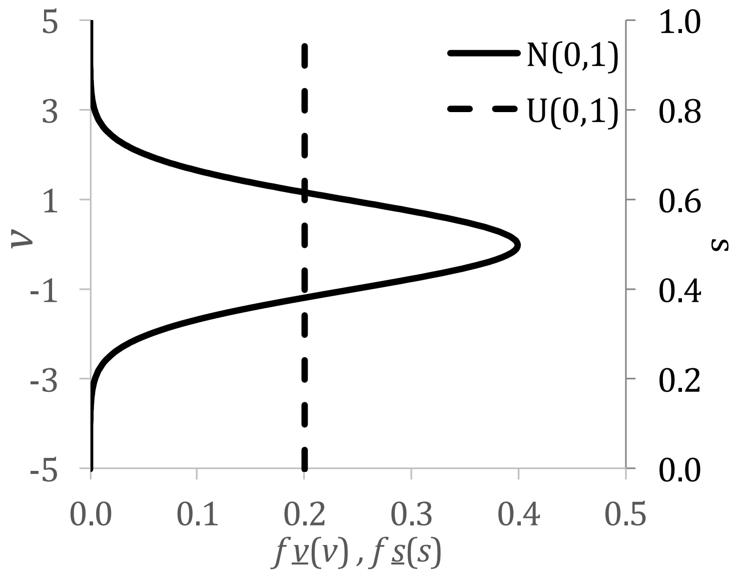

Figure 1: An example of a Gaussian N(0,1) velocity distribution mapped to a uniform U(0,1) location distribution.

2.3. Demonstration of concepts with the one-dimensional von Kàrman profile

The presented methodology described in brief in the previous section has two strong advantages over established approaches of fitting an idealized (uniform flow) deterministic profile directly to observations. Let us assume the profile of the streamwise velocity for discharge estimation across a natural river section. First, since the profile depends entirely on the random variable of the velocity $\underline{v}$ or the location $\underline{s}$, we may choose a convenient distribution $F_{\underline{s}}(s)$, e.g. a uniform one that should require less effort and equipment (see further details in the discussion in sect. 4, and applications and discussion in Dimitriadis et al., 2019b, sect. 3.4). Second, we may even acquire information on the distribution of the longitudinal velocity $F_{\underline{v}}(v)$, following, for example, the framework of maximum entropy under typical hydraulic constraints (see sect. 3; as first shown by Chiu, 1987).

For an illustration of the above methodology, we assume the one-dimensional von Kàrman (1930) profile of the longitudinal velocity on a vertical between the bed and the water surface in an infinitely-wide river cross-section under fully-developed turbulent flow, turbulence being modelled according to the mixing-length theory (Schlichting, 1960; for more generic expressions see e.g., Schlichting, and Gersten, 2017):

$$v = g(y) = \alpha \ln(y/b) \tag{12}$$

where $v = g(y)$ is the velocity profile, y denotes the distance from the bed with $b \leq y \leq h$, h is the total water depth, b is the bed roughness indicating the water depth where the velocity becomes approximately zero, i.e. $g(b) = 0$ (and stays zero until $y = 0$ if the pressure gradient is zero or becomes even negative until brought back to zero at $y = 0$ if a suction at the wall takes place leading to boundary layer separation), and $\alpha = u^*/\kappa$ is the *friction velocity* u^* (in same units as v) divided by the von Kàrman constant κ (usually taken as $\sim$0.4 for clear water).

We then assume that the above profile is unknown and wish to take velocity samples over the entire depth. As mentioned above, we may choose a convenient sampling distribution $F_{\underline{y}}(y)$, such as the uniform one, with y denoting depth measured from the channel bottom:

$$F_{\underline{y}}(y) = \frac{y - b}{d - b} \tag{13}$$

for $b \leq y \leq d$, and $P(y < b\ ) = 0$ and $P(y > d\ ) = 1$.

We generate depths (i.e. sample points) by the above distribution and estimate the velocities from the expression $g(y) = \alpha \ln(y/b)$, as if we had actually measured them in the field. Afterwards, we estimate the probability distribution function of the velocity samples through, for example, a quantile plot (other statistical test may be used) and test what velocity profile optimally fits the data (Fig. 2). Since we *a priori* know the profile, we can estimate the true velocity distribution from the inverse function $y = g^{-1}(v) = b\mathrm{e}^{v/\alpha}$, as:

$$f_{\underline{v}}(v) = f_{\underline{s}}\big(g^{-1}(v)\big)\left|\frac{\mathrm{d}g^{-1}(v)}{\mathrm{d}v}\right| = \frac{b\mathrm{e}^{v/\alpha}}{\alpha(d - b)} \tag{14}$$

which results in

$$F_{\underline{v}}(v) = \frac{e^{v/\alpha} - 1}{d/b - 1} \tag{15}$$

for $0 \leq v \leq \alpha \ln(d/b)$. Note that we here assume the correct distribution, but in case of an unknown profile we should perform statistical test for many functions, in order to decide on the best-fitted one.

Finally, after we decide on the best-fitted distribution, we estimate the velocity profile by solving the nonlinear expression:

$$\left|\frac{\mathrm{d}g(y)}{\mathrm{d}y}\right| = \frac{f_{\underline{y}}(y)}{f_{\underline{v}}(g(y))} = \frac{\frac{1}{d-b}}{\frac{b e^{g(y)/\alpha}}{\alpha(d-b)}} \tag{16}$$

If we assume a positively monotonic profile (the negative profile cannot satisfy both limits at bottom and surface), we have that:

$$\frac{\mathrm{d}(g(y))}{\mathrm{d}y} = \frac{\alpha}{b} e^{-g(y)/\alpha} \tag{17}$$

which after manipulations results in

$$g(y) = \alpha \ln(y) + c \tag{18}$$

with $c = -\alpha \ln(b)$, and so, $g(y) = \alpha \ln(y/b)$, a.k.a. Eq. 12.

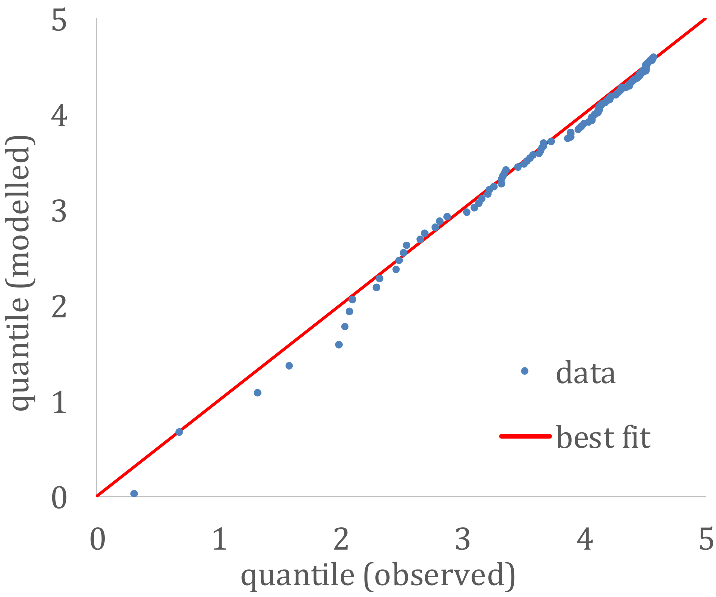

Figure 2: Quantile plot between the n observed velocities (estimated from the one-dimensional von Kàrman velocity profile for α = 1 m/s, b =0.01 m and n = 100), and the modelled velocities estimated from the quantile of the derived velocity distribution function $F_{\underline{v}}^{-1}\big(i/(n+1)\big)$, where i = [1, n] is the increasing index (i.e. from small to large values) assigned to each sorted observed velocity.

We now assume that we know the von Kàrman's profile and we seek the probability distribution of $g(y)$. For variety, we express the von Kàrman profile for a reference level set at the water surface instead of the bottom as previously shown, i.e.:

$$v = g(y) = \alpha \ln(d/b - y/b) \tag{19}$$

where y now denotes the depth measured from the surface with $y_{\mathrm{o}} = 0$ and $y_{\mathrm{m}} = d - b$, and again the maximum velocity is $v_{\mathrm{m}} = \alpha \ln(d/b)$. Note that we may easily alter the profile so that the depth varies from 0 to $y_{\mathrm{m}} = d$, i.e. $g(y) = \alpha \ln((d+b)/b - y/b)$ with now $v_{\mathrm{m}} = \alpha \ln(d/b + 1)$.

For convenience, we formulate the velocity to be positively monotonic with respect to the depth, hence the $\zeta(s)$ function can be expressed as (Fig. 3):

$$\zeta(y) = 2v_{\mathrm{m}} - g(y) \tag{20}$$

where $|\mathrm{d}\zeta(y)/\mathrm{d}y| = |\mathrm{d}g(y)/\mathrm{d}y|$.

For a uniform distribution of sampling, we can now derive the velocity distribution from Eq. 3:

$$f_{\underline{v}}(v) = \frac{d^2}{\alpha b(d-b)}\, \mathrm{e}^{-\frac{v}{\alpha}} \tag{21}$$

which corresponds to the exponential distribution, i.e. $F_{\underline{v}}(v) = 1 - \mathrm{e}^{-v/\alpha}$, with a low and high truncation at v_{m} and $2v_{\mathrm{m}}$, respectively. Note that since the absolute derivatives of $g(y)$ and $\zeta(y)$ are equal both solutions satisfy the velocity distribution, and based on assumptions for the hydraulic conditions we may decide upon which to select (see below).

Due to the adopted hydraulic condition that the actual derivative must be positive, since shear stress is expected to increase with depth, the derived true velocity profile is the original von Kàrman one. Interestingly, if we measure the bed roughness (and assume it remains constant for a long period), the total water depth in the cross-section, and the velocity at surface, we may fully estimate the proposed profile, and thus the streamflow through the velocity mean:

$$\overline{v} = \frac{dv_{\mathrm{m}}}{d-b} - \alpha = \frac{dv_{\mathrm{m}}}{d-b} - \frac{v_{\mathrm{m}}}{\ln(d/b)} \tag{22}$$

and for $d \gg b$ we have $\overline{v}/v_{\mathrm{m}} \approx 1 - 1/\ln(d/b)$.

We remark that Chiu (1988) has also shown how a similar to the above profile in Eqn. 19 can be derived from entropy maximization of a truncated positive-exponential distribution and, in fact, he proposed a more generalized expression to allow zero velocity at zero depth. As we show above in Eqn. 21, the original von Kàrman model can be also derived from a truncated exponential distribution.

Finally, for the pressure and water-depth, it can easily be shown that for a hydrostatic profile $\psi(y) = \omega(y) = y$ and $\overline{p} = \overline{w} = y/2$, where $\overline{p}$ and $\overline{w}$ are the pressure and depth mean values, respectively. The isobaric and depth lines, and the isovels, are obviously parallel to the *x*-*x* axis, i.e. independent of the position *x* within the cross-section.

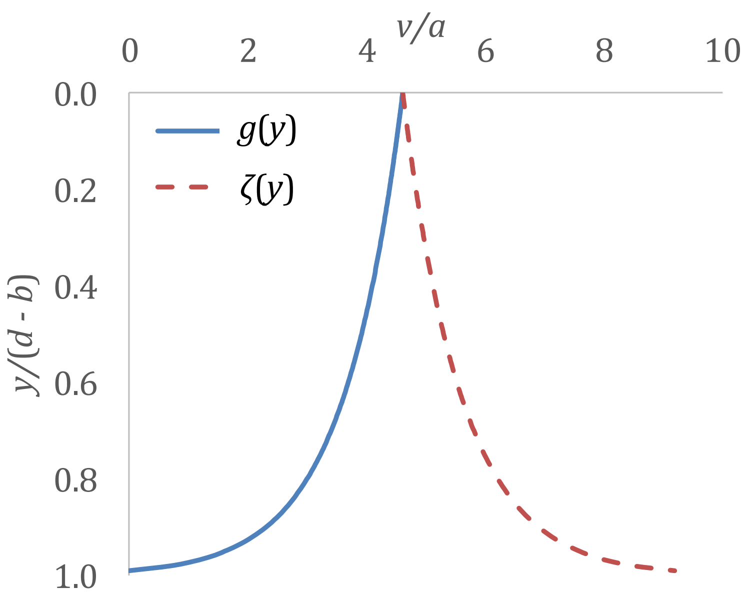

Figure 3: The von Kàrman velocity profile $g(y)$ formulated for depth y measured from the water surface and the transformed profile $\zeta(y)$, so that the velocity monotonically increases with depth.

3. Maximized entropy probability distribution under typical hydraulic constraints

As mentioned previously, there are numerous possible probability distributions that could be used for the above methodology. In this section, we describe how we can introduce hydraulic constraints and thus, derive a generic distribution function for the velocity, pressure and water-depth. We note that there are numerous constraints that one could employ, and therefore it is expected that the resulting distributions will never be exact. Nevertheless, we are interested in narrowing the variability of this inaccuracy to a selected degree and, at the same time, using a small number of parameters. Following Chiu's (1988) methodology, we introduce the most typical, for a natural channel, hydraulic constraints of the conservation of mass, linear momentum rate and energy rate for incompressible steady flow. Then, by following the principle of maximum entropy, we derive general distributions for the variables of interest that satisfy these constraints.

3.1. Maximized information entropy probability distribution

Entropy for the velocity in continuous-time (similarly for the pressure and water-depth) is defined as (Boltzmann, 1877; Gibbs, 1878; and Shannon, 1948; abbreviated BGS, as discussed in Koutsoyiannis, 2011):

$$H(\underline{v}; \boldsymbol{\lambda}) := -\int_{-\infty}^{\infty} f_{\underline{v}}(v; \boldsymbol{\lambda}) \ln\left(f_{\underline{v}}(v; \boldsymbol{\lambda})\right) \mathrm{d}v \tag{23}$$

where $\boldsymbol{\lambda} = [\lambda_0, \lambda_1, \dots, \lambda_m]$, are parameters ($\lambda_m \geq 0$; also known as Lagrangian multipliers of the BGS entropy) linked to m constraints. For example, for constraints based on the first m raw statistical moments we have:

$$\int_{-\infty}^{\infty} v^r f_{\underline{v}}(v; \boldsymbol{\lambda}) \mathrm{d}v = \mathrm{E}\left[\underline{v}^r\right], \text{for } r = 0, 1, \dots, m \tag{24}$$

The resulting distribution, in continuous-time, from the above definitions and constraints is the, so-called, Maximum Entropy Density distribution (MED; Jaynes, 1957):

$$f_{\underline{v}}(v; \boldsymbol{\lambda}) := \mathrm{e}^{-(\lambda_0 + \lambda_1 v + \dots + \lambda_m v^m)} \tag{25}$$

with $\lambda_m > 0$. Note that when v is not (lower or upper) bounded (i.e. $-\infty < x < \infty$), then, for an even number of constraints (i.e. odd number of m) the maximum entropy cannot be reached (Cover and Thomas, 1991, sect. 12.3), while for a bounded variable it exists (see also discussion in sect. 3.3).

The entropy of the location is similarly $H(\underline{s}; \boldsymbol{\lambda}) = -\int_{-\infty}^{\infty} f_{\underline{s}}(s) \ln\left(f_{\underline{s}}(s)\right) \mathrm{d}s$, or simply $H(\underline{s})$, and is linked to that of the velocity $H(\underline{v})$, via the transformation function $\underline{v} = g(\underline{s})$. It can be easily shown that:

$$H(\underline{v}) = H(\underline{s}) + \int_{-\infty}^{\infty} f_{\underline{s}}(s) \ln\left(\left|\frac{\mathrm{d}g(s)}{\mathrm{d}s}\right|\right) \mathrm{d}s \tag{26}$$

where we set $\theta := \int_{-\infty}^{\infty} f_{\underline{s}}(s) \ln\left(\left|\frac{\mathrm{d}g(s)}{\mathrm{d}s}\right|\right) \mathrm{d}s$.

Note that the constraints of $H(\underline{s})$ are the same as those of $H(\underline{v})$, but expressed through the transformation function $\underline{v} = g(\underline{s})$. For example, if the constraints are the raw moments of the velocity, then the constraints for the location variable are $\mathrm{E}[g^r(\underline{s})]$, and thus, the resulting distribution function of the location variable is:

$$f_{\underline{s}}(s; \boldsymbol{\lambda}) := \mathrm{e}^{-\left(\lambda_0 + \lambda_1 g(s) + \dots + \lambda_m g^m(s) - \ln\left(\left|\frac{\mathrm{d}g(s)}{\mathrm{d}s}\right|\right)\right)} \tag{27}$$

3.2. Typical hydraulic conditions and statistical constraints

We consider one-dimensional and incompressible steady-flow conditions for the random variables of the longitudinal velocity, pressure and water-depth all spatially varying within a cross-section. We set the reference level for the sampling location, velocity, pressure and water-depth variables at the cross-section surface, i.e. at the point(s) with minimum distance from atmospheric pressure level for the open-channel flow case or at the soffit of the cross-section for the pipe flow case.

Note that the water-depth and location variables can sometimes coincide, as in one-dimensional analysis, but we stress that they are different. For example, as we show below, while the location variable is always assumed to be uniformly distributed, since it is uniformly mapped to the cross-section, the water-depth may follow other distributions. Therefore, the location variable varies from a fixed low value $s_o = 0$ on the boundary with the smallest distance from the origin to some maximum s_m on the boundary with the largest distance from the origin (e.g. $s_{\mathrm{m}} = d$ in open-channel flows, and fixed $s_{\mathrm{m}} = D$ in circular pipe flows, where D is its diameter). Similarly, the velocity varies from a low value v_o at the wall boundaries (e.g., $v_o = 0$ for the no-slip condition) to some maximum value v_{m} located usually at the point with the maximum distance from boundaries (e.g., free-surface for rectangular open-channel flows and pipe centre for circular pipe flows). Similarly, the pressure varies in a positively monotonic way with respect to depth from a fixed small value p_o, usually at the highest point of the cross-section (e.g., $p_o = 0$ at the water surface in open channels; $p_o > 0$ at the section soffit in pipe flows) to some maximum value p_{m} at the lowest point of the cross-section. Finally, the water-depth varies from a zero value $w_o = 0$ at the water surface to some maximum value w_{m} at the vertical with the largest distance from surface. We note that in fixed geometries, as for example in pipe flows, the water-depth can be again defined with respect to the pipe soffit (see application in the companion work of Dimitriadis et al., 2019b sect. 3.2). However, these geometries are of no particular interest for the water-depth analysis in this study, which mostly focuses on naturally-formed cross-sections and not strictly man-made.

The values of the above variables at the boundaries are either fixed to a theoretically derived or observed value such as zero (e.g. $s_o = 0$, $v_o = 0$, $p_o = 0$, and $w_o = 0$) or other values (e.g. $s_{\mathrm{m}} = D$) or are left unbounded until observed. For example, there is no hydraulic condition or other physical justification preventing a water lump to reach arbitrarily high values (see discussion for the velocity in Lighthill and Whitham, 1955) and so, it would be redundant to assume that a maximum value within a natural cross-section is imposed by nature. Exceptions may include laboratory or other experiments where the maximum boundary values of depth, velocity and pressure are specified by the observer for the specific experiment. A rather trivial information is that the speed of sound is considered to be the physical limit of water wave velocity, while for the other two is the height of the atmospheric boundary layer, but for the examined cases, the effect of bounding these variables to these limits or leaving them unbounded is assumed negligible. We note that leaving these variables unbounded does not imply that their maximum values in a cross-section could reach high magnitudes. However, if their values at the boundaries are observed, fixed or specified, then we may pass this information as a constraint for the entropy maximization. If no information is available, then we may simply draw a sample series from the distribution of the unbounded maximized entropy variable of interest, with the only constraint to be positive or even totally unbounded in cases where velocity can be negative, and then, employ hydraulic conditions to re-arrange the sample values in the cross-section. In other words, the unobserved, unfixed or unspecified boundary values are required in the deterministic re-construction model and not in the probabilistic one. For example, in case of pipe flow, the depth is bound to the fixed geometry, while the velocity and pressure are only low-bounded to zero (i.e. positive value), since the maximum velocity and pressure magnitudes are no longer fixed and may change based on different discharges, wall-roughness and flow-states.

Fortunately, in common cross-sections, the values at boundaries can be practically assumed or accurately measured by non-invasive methods, as for example from drones and acoustic or pulse recording devices (e.g., Sasso et al., 2018). An alternative approach for estimating these boundary values is implicitly by the maximum depth in the cross-section, which is the easiest measurable variable. Such methods may be employed through either hydraulic approaches such as the Manning formula (e.g., Dimitriadis, 2018), or the rating curve (e.g., Manfreda, 2018), or even via computational fluid dynamic simulations in case there is no information for the examined area (e.g., Dimitriadis et al., 2016b). In any case, we should avoid estimating these values by the maximum value drawn from a sample, which is a highly biased estimation, since it is obviously explicitly determined by the most extreme value of the sample.

Based on the above configuration, we map the velocity, pressure and depth distributions on the fixed area of the cross-section through the Monte-Carlo technique (Metropolis, 1989) that assumes a uniform sampling distribution $f_{\underline{s}}(s)$ to estimate the integral over the area A of any continuous function $\Theta(s)$ with fixed values at the boundaries of the area. Specifically, it can be shown that if we generate a number of N points at locations s_i ($i = 1, \dots, N$) uniformly distributed within the cross-section, and estimate the function values $\Theta(s_i)$, then:

$$\int_A \Theta(s)\mathrm{d}A = \lim_{N\to\infty} \sum_{i=1}^{N} \Theta(s_i) \approx A\mathrm{E}\left[\hat{\Theta}\left(\underline{s}\right)\right] \tag{28}$$

where $\hat{\Theta}(s_i) = 1/N \sum_{i=1}^{N} \Theta(s_i)$ is an estimator for the function $\Theta(s)$, which is unbiased, and thus,

$$1/A \int_A \Theta(s)\mathrm{d}A \approx \mathrm{E}\left[\Theta\left(\underline{s}\right)\right] = \int_{-\infty}^{\infty} \Theta(s) f_{\underline{s}}(s)\mathrm{d}s \tag{29}$$

Then, it can be easily shown that for the velocity (similarly for the other variables):

$$P\left(\underline{v} \le v_{\mathrm{h}}\right) - P\left(\underline{v} \le v_{\mathrm{l}}\right) = P\left(\underline{s} \le \zeta^{-1}(v_{\mathrm{h}})\right) - P\left(\underline{s} \le \zeta^{-1}(v_{\mathrm{l}})\right) \approx 1/A \int_{\zeta^{-1}(v_{\mathrm{l}})}^{\zeta^{-1}(v_{\mathrm{h}})} \mathrm{d}A \tag{30}$$

where v_{l} and v_{h} are two arbitrary lower and higher velocity values mapped at the locations $\zeta^{-1}(v_{\mathrm{l}})$ and $\zeta^{-1}(v_{\mathrm{h}})$, respectively, which are essentially the locations of the original monotonic velocities before the hydraulic conditions take place and transform them to the final non-monotonic ones.

In other words, the occurrence probability of a range of velocities (between v_l and v_h) equals the percentage area between the locations $\zeta^{-1}(v_\mathrm{l})$ and $\zeta^{-1}(v_\mathrm{h})$, where these velocities are generated with the Monte-Carlo uniform sampling in the area. Caution is required when one changes the sampling distribution to a non-uniform one with respect to the location, since, obviously, this would result in a different estimation of the above integral (see an application in the companion work of Dimitriadis et al., 2019b, sect. 3.4). In fact, if one samples a function $\Theta(y)$ uniformly in an area with respect to the variable ξ instead of the location variable s, then, if these are for example, connected along a vertical line y through the function $\xi = g(y) \neq y$, then:

$$\int_{y_\mathrm{o}}^{y_\mathrm{m}} \Theta(y)\mathrm{d}y = \int_{g^{-1}(\xi_\mathrm{o})}^{g^{-1}(\xi_\mathrm{m})} \frac{\mathrm{d}g^{-1}(\xi)}{\mathrm{d}\xi} \Theta(\xi)\mathrm{d}\xi \neq \int_{\xi_\mathrm{o}}^{\xi_\mathrm{m}} \Theta(\xi)\mathrm{d}\xi \tag{31}$$

where equality holds only when $g(y) = y$. Note that if one value of ξ corresponds to two or more location points of s then the sign $>$ applies to the above expression, while if one location point s corresponds to two or more values of ξ then the sign $<$ applies instead.

After mapping the distributions of velocity, pressure and depth to the uniform one for the location variable, we can truncate them to their determined (observed, fixed or specified) values on the boundaries, as mentioned above.

Based on the above concepts, we can now express the hydraulic conditions for the three variables through the incompressible one-dimensional steady-state dynamics. The three typical hydraulic conditions for the longitudinal velocity (Chiu, 1989), pressure and depth of a cross-section involve the conservation of mass, linear momentum rate and energy rate.

An extra fundamental hydraulic and statistical condition is that:

$$\int_{-\infty}^{\infty} f_{\underline{v}}(v)\mathrm{d}v = \int_{p_\mathrm{o}}^{p_\mathrm{m}} f_{\underline{s}}(p)\mathrm{d}p = \int_{s_\mathrm{o}}^{s_\mathrm{m}} f_{\underline{s}}(s)\mathrm{d}s = \frac{1}{A}\int_A \mathrm{d}A = 1 \tag{32}$$

where A can be linked to the s_o and s_m values if the geometry of the cross-section is assumed knowable.

For the mean cross-sectional velocity, it can easily be shown that the conservation of mass holds:

$$\mathrm{E}[\underline{v}] = \int_{-\infty}^{\infty} v f_{\underline{v}}(v)\mathrm{d}v = \frac{1}{A}\int_A g(s)\mathrm{d}A = Q/A = \overline{v} \tag{33}$$

where Q the discharge, which can be linked to the expected value of the velocity as $\mu = Q/A$.

Similarly, the mean linear momentum rate for the cross-section in the flow direction is $\lambda PA + \rho\beta Q^2/A$, where P is the mean hydrostatic pressure (in Pa) exerted at the pressure centroid, and λ is the pressure parameter (Yen, 1973; similar analysis in Koussis, 1975), which is defined through:

$$\mathrm{E}\left[\underline{p}\right] = \int_0^\infty p f_{\underline{p}}(p)\mathrm{d}p = \frac{1}{A}\int_A \psi^2(s)\mathrm{d}A = \lambda P = \overline{p} \tag{34}$$

The pressure centroid $p_\mathrm{c} = \frac{1}{A w_\mathrm{c}}\int_A s\psi(s)\mathrm{d}A$ is a function of the area centroid w_c, i.e.:

$$\mathrm{E}[\underline{w}] = \int_0^\infty w f_{\underline{w}}(w)\mathrm{d}w = \frac{1}{A}\int_A \omega(s)\mathrm{d}A = \overline{w} \tag{35}$$

and the second-moment, i.e.:

$$\mathrm{E}[\underline{w}^2] = \int_0^\infty w^2 f_{\underline{w}}(w)\mathrm{d}w = \frac{1}{A}\int_A \omega^2(s)\mathrm{d}A = \frac{\delta}{A}\int_A s\psi(s)\mathrm{d}A \tag{36}$$

where $\delta = \mathrm{E}[\underline{w}^2]/(w_c p_c)$ is a pressure-centroid coefficient that can be determined if the pressure profile and the geometry of the cross-section are known. Clearly, for a hydrostatic profile, $\lambda = \delta = 1$. Note that since the pressure centroid includes the location variable, the above centroids can be also expressed through the first and second statistical moments of pressure. Interestingly, the latter expression can be also regarded as the cross-correlation between pressure and depth. Similarly, the velocity centroid could be defined and simulated but since this is not directly included in the conservation of the momentum rate, it can be neglected. Also, for the pressure parameter, Ohtsu et al. (2004) proposed an expression through the cross-correlation between velocity and pressure. However, as shown in the companion work of Dimitriadis et al. (2019b, sect. 3.1.3 and 3.3), for typical flows the effect of conserving or not the pressure centroid through the first two moments of pressure or depth, does not significantly alter their profiles.

If we assume a hydrostatic pressure model then, both magnitudes can be explicitly estimated through only p_o and p_m. In fact, the hydrostatic profile emerges when the probability distributions of both are linearly linked through $\underline{w} = (\underline{p} + p_\mathrm{o})/(\gamma\cos\varphi)$, where $\gamma = \rho g$ and $\cos\varphi$ is the local channel slope. For example, in a rectangular cross-section of width w and depth d, $P = \gamma w d^2/2/\cos\varphi$ exerted at $w_\mathrm{c} = d/2/\cos\varphi$, with $p_\mathrm{c} = 2d/3/\cos\varphi$ measured from surface. However, in the general case that we examine here, we have no information on the pressure profile; and are interested in conserving its mean value and centroid. We note that the effect of the force caused by gravity and the mean shear stress at an infinitely thin cross-section is assumed negligible compared to the other forces.

Therefore, for the linear momentum rate to be fully conserved, we must also conserve β (since water density ρ is considered fixed), which is linked to the second-order raw moment of velocity:

$$\mathrm{E}[\underline{v}^2] = \int_0^\infty v^2 f_{\underline{v}}(v)\mathrm{d}v = \frac{1}{A}\int_A g^2(s)\mathrm{d}A = \beta\left(\mathrm{E}[\underline{v}]\right)^2 \tag{37}$$

where $\beta \geq 1$ is the, so-called, Boussinesq (1877) coefficient (Chanson, 1999), and is linked to the coefficient of variation $C_{\mathrm{v}} = \sigma/\mu = \sqrt{\left(\mathrm{E}[\underline{v}^2] - (\mathrm{E}[\underline{v}])^2\right)}/\mathrm{E}[\underline{v}] = \sqrt{\beta - 1}$, with σ the standard deviation of the velocity, i.e. $\sigma = \sqrt{\mathrm{E}\left[(\underline{v} - \mu)^2\right]}$.

Finally, the mean total energy transfer rate (power) for the cross-section is $\rho g Q \left(Z + \frac{\lambda P}{\gamma} + \frac{\alpha}{2g} Q^2/A^2 + \varepsilon\right)$; this can be conserved through again the mean pressure height, which is linked to the absolute pressure divided by γ, and the mean potential energy height Z, which equals the area centroid $\overline{w}$ that is already conserved through the linear momentum rate. Again, only for a hydrostatic profile the sum of the mean potential energy height and the pressure heights is constant and equal to p_{m}.

The coefficient α is linked to the third-order raw moment of velocity:

$$\mathrm{E}[\underline{v}^3] = \int_0^\infty v^3 f_{\underline{v}}(v)\mathrm{d}v = \frac{1}{A}\int_A g^3(s)\mathrm{d}A = \alpha(\mathrm{E}[\underline{v}])^3 \tag{38}$$

where $\alpha \geq 1$ is the, so-called, Coriolis (1836) coefficient (Chanson, 1999), and can be linked to the coefficient of skewness $C_{\mathrm{s}} = k/\sigma^3 = \left(\mathrm{E}[\underline{v}^3] - 3\mu\mathrm{E}[\underline{v}^2] + 2\mu^3\right)/(\mu C_{\mathrm{v}})^3 = (2 + \alpha - 3\beta)/(\beta - 1)^{3/2}$ or $C_{\mathrm{s}} = \left(\alpha - 1 - 3{C_{\mathrm{v}}}^2\right)/{C_{\mathrm{v}}}^3$, with k the skewness of the velocity, i.e. $k = \mathrm{E}[(\underline{v} - \mu)^3]$. Note that for large variability coefficient with $C_{\mathrm{v}} > \sqrt{(\alpha - 1)/3}$ we have that $C_{\mathrm{s}} < 0$, while in case of a symmetrical probability distribution of velocity, i.e. $C_{\mathrm{s}} = 0$, we have that $\alpha = 3\beta - 2 \geq \beta$. Interestingly, Rahimpour (2017) has shown that in rectangular channels this expression approximately holds, and so, the velocity distribution can be well approximated in typical scenarios by a Gaussian distribution (see also conclusions in Dimitriadis et al., 2019; 2019b).

One may also approximate the energy losses based on empirical expressions, such as the Manning (for open-channels) or the Darcy-Weisbach (for pipe flow) equations, which depend on parameters explicitly determined by variables such as the area of the cross-section, the Reynolds number (e.g., for the friction coefficient in pipe flow) or the ratio of the square root of the energy slope over the Manning roughness coefficient (in open-channel flow). Note that although implicit models also exist for the Boussinesq and Coriolis parameters (e.g., Temple, 1986), here we wish to preserve them explicitly through the velocity distribution under the discussed methodology.

Since here we are interested in the absolute value of the spatial velocity derivative (i.e., with respect to location) there is no need to add parameters related to the magnitude and location of the maximum velocity. After estimating the velocity derivative, we may adopt reasonable assumptions on the flow conditions and on the shear stress and estimate the actual value of the velocity, and thus, its profile. For example, for ordinary cases of open-channel flows or pipe flows the flow conditions are expected to be turbulent (and thus, the momentum and energy coefficients may be assumed constant, e.g. close to 1, for a large variety of streamflow), and the velocity is expected to increase when moving away from boundaries due to the decrease of the shear stress initiated by the water viscosity and friction (e.g., Guo and Julien, 2005). In flows where only one boundary parallel to the flow exists (e.g., channels with large width to depth ratio), the derivative of the velocity with respect to the distance from the boundaries is always positive, and thus the maximum velocity occurs at the water surface. However, in cases where the effects from the shear stress cannot be ignored at the water surface (e.g., Rajaratnam and Muralidhar, 1969) or at the side boundaries (e.g. channels with small width to depth ratio or pipes; Yang et al., 2004), the maximum velocity will occur below the surface for an open-channel or close to the center for a pipe flow. Since we assume that the velocity and location are defined in such a way to be bijective, the maximum velocity and its location in the cross-section can be easily determined by the velocity and corresponding location where the ratio of their probability distributions functions is maximized (see applications in the companion work of Dimitriadis et al., 2019b, sect. 3.1.2, 3.2 and 3.3).

3.3. Probability distributions for the longitudinal velocity, pressure and depth under entropy maximization

As shown in the previous section, the one fundamental and the three typical hydraulic conditions for the one-dimensional analysis of a natural river correspond to the conservation of the expected, variance and skewness values of the longitudinal velocity, the expected (and variance) of the depth and pressure height, provided that the energy losses can be explicitly determined by the remaining values. Other cases may involve the need to conserve additional quantities as for example the angular momentum or vorticity. In such cases, additional parameters must be introduced related to the variables of interest.

Therefore, the maximized entropy probability distribution for the pressure height and water-depth result in the exponential distribution (abbreviated ME1; where $\lambda_m = 0$ for $m > 1$, $\lambda_1 > 0$) or, in cases where the pressure centroid is important to be conserved, to the lower-tail truncated (for $w, p > 0$) Gaussian one (abbreviated ME2; where $\lambda_m = 0$ for $m > 2$). The resulting distribution for the velocity is the three-parameter maximized entropy distribution (abbreviated ME3; where $\lambda_3 > 0$). In cases where the discharge (or equivalently the average area and velocity) tends to very large values (theoretically to infinity), the distribution of the depth and the velocity tends to the uniform distribution (abbreviated as ME0; where $\lambda_0 = \ln(v_\mathrm{m} - v_\mathrm{o})$ and $a = \beta = 1$ for the velocity). When $C_\mathrm{v} = 1$, the velocity distribution is the ME1 (with $\beta = 2$ and $a = 6$), while when $C_\mathrm{v} < \sqrt{\pi/2 - 1}$, the velocity distribution is the lower-tail truncated (for $v > 0$) Gaussian distribution (where $\lambda_m = 0$ for $m > 2$), respectively (for intermediate values of the C_v the distribution is *J*-shaped between the two; Koutsoyiannis, 2005). We note that in case no constraints are conserved for the depth and velocity the derived velocity profile is the one-dimensional plane Couette flow, i.e. $v = v_m(1 - y/d)$, that corresponds to the laminar flow of a viscous fluid (i.e., constant shear stress along the vertical) between two parallel plates, one of which is moving relative to the other with v_m (e.g., Case, 1960).

In all the above cases, the location variable follows the uniform distribution ME0, i.e.:

$$F_{\underline{s}}(s) = \frac{s - s_o}{s_m - s_o} \tag{39}$$

The exponential probability density distribution for the velocity (ME1) low-truncated at zero (i.e., no-slip boundary condition) is (similarly for pressure and depth):

$$f_{\underline{v}}(v) = \mathrm{e}^{-\lambda_0 - \lambda_1 v} \tag{40}$$

where $\mu = \mathrm{E}[\underline{v}]$, $\lambda_0 = \ln(\mu)$ and $\lambda_1 = 1/\mu$, while $\lambda_0 = \ln\left(\left(1 - \mathrm{e}^{-\lambda_1 v_\mathrm{m}}\right)/\lambda_1\right)$ and $\mu = v_\mathrm{m}/\left(1 - \mathrm{e}^{-\lambda_1 v_\mathrm{m}} - 1/\lambda_1\right)$ for the higher-tail truncated distribution at v_m (see also Chiu, 1989).

The low-truncated Gaussian distribution for the velocity (ME2), when conserving the first two constraints, is (similarly for pressure and depth):

$$f_{\underline{v}}(v) = \frac{\varphi(v; \mu', \sigma')}{1 - \Phi\left(\frac{v_\mathrm{o} - \mu'}{\sigma'}; \mu', \sigma'\right)} \tag{41}$$

where μ' and σ' are the mean and standard deviation without the truncation effect, $\varphi(v; \mu', \sigma') = \mathrm{e}^{-((v-\mu')/\sqrt{2\sigma'^2})^2}/\sqrt{2\pi\sigma'^2}$ is the Gaussian density distribution function, $\Phi(x) = 1/2 + 1/2\left(\mathrm{erf}\left((x - \mu')/\sqrt{2\sigma'^2}\right)\right)$ is the probability distribution function at x, $\mathrm{erf}(x) = \int_{-x}^{x} \mathrm{e}^{-t^2} \mathrm{d}t/\sqrt{\pi}$ is the error function, while the mean, variance, skewness and the corresponding λ_0, λ_1 and λ_2 can be found in Koutsoyiannis (2005; supplementary material). For the unbounded velocity (e.g., in cases where the velocity can be negative) and high-truncated distributions (maximum velocity is either observed, fixed or specified), we set $\Phi((v_\mathrm{o} - \mu')/\sigma')$ to 0, and 1 to $\Phi((v_\mathrm{m} - \mu')/\sigma')$, respectively.

The ME3, when conserving all three constraints for the velocity, is $f_{\underline{v}}(v) = \mathrm{e}^{-(\lambda_0 + \lambda_1 v + \lambda_2 v^2 + \lambda_3 v^3)}$, which exists only for a low-truncated variable at v_o. We may employ this density distribution by estimating the Lagrangian multipliers through an indirect approach rather than through the traditional Newton-Raphson numerical approximations (Mead and Papanicolaou, 1984; Rockinger and Jondeau, 2002; Santana et al., 2006). Since the ME3 is difficult to handle (see also the analysis and application in Kumbhakar et al., 2019a), we may employ a flexible three-parameter version of the Pareto-Burr-Feller distribution (PBF; see discussion and references in Koutsoyiannis et al., 2018), which is found to adequately describe several processes varying from local turbulent scales (e.g. Dimitriadis et al., 2016) to hydrometeorological scales (Dimitriadis, 2017; Dimitriadis and Koutsoyiannis, 2018) and is also linked to the entropy maximization under the first three generalized K-moments (Koutsoyiannis, 2020). At the end, we may fit the fitted PBF to the ME3 and implicitly estimate its parameters (see application in Dimitriadis et al., 2019b, sect. 3.1.2). The examined version for $v > 0$ is also known as Pareto IV or BurrXII distribution and its probability distribution function is:

$$F_{\underline{v}}(v) = 1 - \left(1 + (v/p_1)^{p_2}\right)^{-p_3} \tag{42}$$

where $\mathrm{E}[\underline{v}] = p_1 \Gamma(p_3 - 1/p_2)\Gamma(1 + 1/p_2)/\Gamma(p_3)$, $\mathrm{E}[\underline{v}^2] = p_1{}^2 \Gamma(p_3 - 2/p_2)\Gamma(1 + 2/p_2)/\Gamma(p_3)$ and $\mathrm{E}[\underline{v}^3] = p_1{}^3 \Gamma(p_3 - 3/p_2)\Gamma(1 + 3/p_2)/\Gamma(p_3)$, and the density distribution can be easily derived from $f_{\underline{v}}(v) = \mathrm{d}F_{\underline{v}}(v)/\mathrm{d}v$. For the truncation of this distribution at v_m, we divide the distribution and density function with $F_{\underline{v}}(v_\mathrm{m})$.

We observe that the ME3 distribution (similarly the PBF) has three parameters, same as the proposed approach for the dip-phenomenon in Chiu (1988), but it additionally conserves explicitly the velocity variance and skewness, whereas the established approach implicitly simulates their effects through the parameters of the maximum velocity magnitude and location in the cross-section.

A final remark is that a difficulty of the presented formulation for the velocity is to estimate the first three raw moments based on the monotonic function $\zeta(\underline{s})$, so that the three raw moments for the $g(\underline{s})$ are correctly conserved. The formulation for the water-depth is easier to perform due to its monotonic behaviour. Finally, while in most cases, the pressure varies also monotonically with depth, in the companion work of Dimitriadis et al. (2019b, sect. 3.1.3), an application is shown where pressure is not monotonic, due to presence of a cavity.

To conclude the proposed methodology for deriving the velocity, pressure and water-depth profiles consists of the following steps (several applications are shown for all variables in the companion work of Dimitriadis et al., 2019b):

- The reference level and axis origin are set in such way so that the variables of interest increase in a positive or negative monotonic behaviour with respect to the location. For the pressure and water-depth and for open-channel flows they are usually set at the water surface and at the vertical passing from the centroid of the cross-section area, while for pipe flows the reference level is set at the soffit of the pipe coinciding with the axis origin. For the velocity it can be set at the location with the smallest effect from boundaries, which is usually at the point where the maximum velocity is expected to occur. We stress that the latter location depends only on the selected velocity distribution and the geometry of the cross-section.
- For the pressure and depth, we assume the ME1 or ME2 distributions for typical flow conditions, while for the velocity we assume either the ME0, ME1, ME2 or ME3, depending on how many raw moments we wish to conserve.
- The absolute spatial derivatives of the inverse functions for the velocity, pressure and depth can be derived from Eq. 6, whereas the solution for the function $\zeta(s)$, $\psi(s)$ and $\omega(s)$, respectively, for a uniform sampling distribution is given by Eqn. 7 or 8.
- Depending on the type of flow we decide upon the monotonic or non-monotonic solutions of the previous step. For example, in common type flows (e.g., open-channel with large width-to-depth ratio and pipes) shear stress is expected to increase with respect to depth. In case two (or more) monotonic areas of the derivative exist (e.g., as in the dip-phenomenon), based on the previous assumption, shear stress should reach a maximum value and then follow a trend with a different sign than before the location of its maximum.
- Based on the observed, fixed, specified or unbounded values of the variables at boundaries, we derive the requested profiles for the velocity $g(s)$, pressure $p(s)$ and depth $w(s)$, by appropriately formulating $\zeta(s)$, $\psi(s)$ and $\omega(s)$, based on the assumption(s) of the previous step (e.g., see Eqs. 9-11 for non-monotonic cases).

4. Conclusions

In this study, we are interested in the streamwise velocity, pressure and water-depth spatial deterministic profiles in a cross-section under incompressible one-dimensional steady flow dynamics. For this, we revisit the probabilistic-deterministic framework of Chiu (1988), where the profiles can be determined if the above variables are treated as random. We particularly focus on the absolute values of the spatial derivatives of the three variables with respect to the spatial location, also treated as random, and we show how their values can be linked to the probability distribution functions of the actual variables. We then derive the distributions of the latter based on the assumption of monotonic behaviour and on the principle of entropy maximization with typical hydraulic conditions and statistical constraints implemented in one-dimensional steady flow analysis (i.e. conservation of mass, linear momentum rate and energy rate in a cross-section). The implemented distribution for the spatial location is the uniform one, and the derived distributions for the pressure and water-depth are the exponential or the Gaussian one, and for the velocity a three-parameter one, which is discussed how it can be approximated well by the flexible Pareto-Burr-Feller distribution. Finally, we demonstrate how to derive the actual profiles from the above distributions. A limitation of the proposed methodology is that sometimes the derived profiles can be too complicated to express through analytical formulas and can be only numerically approximated, especially when the additional variance and skewness constraints are used.

Through theoretical arguments, we show that the above configuration exhibits several advantages as compared to the established analysis, where the variables themselves are explicitly analysed and not through their absolute derivatives. Specifically, we discuss how the velocity profile can be constructed without any knowledge on the isovels. Moreover, we show how the original von Kàrman profile can be derived from the maximization of entropy based on some reasonable assumptions on the absolute spatial derivative of velocity. Furthermore, we present a methodology for determining the position of the maximum velocity along a vertical, which may not be located at the water surface (so-called dip-phenomenon) without including an explicit model parameter for it. In the companion work of Dimitriadis et al. (2019b), we show applications where this phenomenon can be simulated by the probability distribution of the velocity through the parameters related to the variance and skewness.

Obviously, by increasing the deterministic constraints (i.e. information) we have on the velocity, pressure and depth profiles, the results will be closer to reality. However, the probabilistic-deterministic framework, as compared to the traditional purely-deterministic ones, can practically handle the effects at the flow from the so-called temporal and spatial random fluctuations of the velocity (e.g. Reynolds stresses), pressure and depth as well as from other sources of uncertainty (e.g. sampling errors), it can maximize the effect on the flow from each known and observed information in the form of hydraulic conditions and statistical constraints, and it is easier to implement.

Acknowledgements

The authors acknowledge the funding from the Hellenic General Secretariat for Research & Technology, under the National Strategic Reference Framework (2014-2020), for the project HYDRO-NET: Hydro-Telemetric Networks of Surface Waters: Gauging instruments, smart technologies, installation and operation, as a part of the Hellenic Integrated Marine and Inland Water Observing, Forecasting and Offshore Technology System, HIMIOFoTS (MIS5002739).

References

Araujo, J.C., and Chaudhry, F.H., Experimental evaluation of2-D entropy model for open-channel flow, *J. Hydraul. Eng.*, 124(10),1064–1067, 1998.

Baldassarre, D.G., and A. Montanari, Uncertainty in river discharge observations: A quantitative analysis, *Hydrol. Earth Syst. Sci.*,13(6),913–921, 2009.

Barbe, D.E., Cruise, J.F., and Singh, V.P., Solution of three-constraint entropy-based velocity distribution, *J. Hydraul. Eng.*,117(10), 1389–1396, 1991.

Barbe D.E., Cruise J.F., Singh V.P., *Derivation of a Distribution for the Piezometric Head in Groundwater Flow Using Entropy*, In: Hipel K.W. (eds) Stochastic and Statistical Methods in Hydrology and Environmental Engineering. Water Science and Technology Library, vol 10/4. Springer, Dordrecht, 1994.

Bechle, A. J., and C.H. Wu, An entropy-based surface velocity method for estuarine discharge measurement, *Water Resour. Res.*,50,6106–6128, doi:10.1002/2014WR015353, 2014.

Benjamin, J.R., and Cornell, C.A., *Probability, statistics, and decision for civil engineers*, Courier Corporation, 2014.

Bogue, D.C. and A.B. METZNER, Velocity Profiles in Turbulent Pipe Flow -Newtonian and Non-Newtonian Fluids, *Industrial & Engineering Chemistry Fundamentals*, 2, 143, 1963.

Boltzmann, L, Über die Beziehung zwischen dem zweiten Hauptsatze der mechanischen Wärmetheorie und der Wahrscheinlichkeitsrechnung respektive den Sätzen über das Wärmegleichgewicht, *Wien. Ber.*, 76, 373–435, 1877. [In German]

Boussinesq, J.V, *Essay on the Theory of Water Flow*, Paris, France, 23, Ser. 3, No. 1, supplement 24, 1-680, 1877 (in French).

Case, K.M., *Physics of Fluids*, 3, 149, 1960.

Chanson H., *The Hydraulics of Open Channel Flow*, Arnold publishers, Wiley: Paris-New York, 1999.

Chen, Y. C., and C. L. Chiu, An efficient method of discharge measurement in tidal streams, *J. Hydrol.*, 265(1–4), 212–224, 2002.

Chen, Y.C., and C.L. Chiu, A fast method of flood discharge estimation, *Hydrol. Processes*,18, 1671–1684, 2004.

Chen, Y.C., and S.P. Kao, Velocity distribution in open channels with submerged aquatic plant, *Hydrol. Processes*, 25(13), 2009–2017, 2011.

Chen, Y. C., Yang, T. M., Hsu, N. S., and Kuo, T. M., Real-time discharge measurement in tidal streams by an index velocity, *Environ. Monit. Assess.*, 184(10), 6423–6436, 2012.

Chen, Y.C.; Hsu, Y.C.; Kuo, K.T., Uncertainties in the Methods of Flood Discharge Measurement,

Water Resour. Manag., 27, 153–167, 2013.

Chiu C.L., Application of Probability and Entropy Concepts in Hydraulics, *Journal of Hydraulic Engineering*, 113: 583-599, 1987.

Chiu, C.L., Entropy and 2-D velocity distribution in open channels, *J. Hydr. Engrg.*, ASCE, 114(7), 738-756, 1988.

Chiu, C.L., Velocity distribution in open channel flow, *J. Hydraul. Engng.*,115, 576-594, 1989.

Chiu, C.L., Application of entropy concept in open channel flow study, *J. Hydr. Engrg.*, ASCE, 117(5), 615-628, 1991.

Chiu, C.L., and Lin, G.F., Computation of 3-D flow and shear in open channels., *J. Hydr. Engrg.*, ASCE, 109(11), 1424-1440, 1983.

Chiu, C.L., and Chiou, J.D., Structure of 3-D flow in rectangular open channels, *J. Hydr. Engrg.*, ASCE, 112(11), 1050-1068, 1986.

Chiu, C.L. and Murray, D.W., Variation of velocity distribution along nonuniform open-channel flow, *J. Hydraul. Engng.*, 118(1), 989-1001, 1992.

Chiu, C.L. and Said, C.A., Maximum and mean velocities and entropy in open-channel flow, *J. Hydraul. Engng.*, 121(1), 26-35, 1995.

Chiu, C.L., and Tung, N.C., Maximum velocity and regularities in open-channel flow, *J. Hydraul. Eng.*,128(4), 390–398, 2002.

Chiu, C.-L., and S.-M. Hsu, Probabilistic approach to modeling of velocity distributions in fluid flows, *J. Hydrol.*,316, 28–42, 2006.

Chiu, C.-L., Lin, G.-F., and Lu, L.-M., Application of probability and entropy concepts in pipe flow study. *J. Hydraul. Eng.*, 119(6),742–756, 1993.

Chiu, C.L., Hsu, S.M., and Tung, N.C., Efficient methods of discharge measurements in rivers and streams based on the probability concept, *Hydrol. Processes*, 19, 3935–3946, 2005.

Choo, Y.M., G.S. Yun, T.H. Choo, Y.B. Kwon, and S.Y. Sim, Study of shear stress in laminar pipe flow using entropy concept, *Environmental Earth Sciences*, 76(17), 616, 2017.

Coriolis, G.G., On the establishment of the formula giving the backwater curves and on the correction to be introduced to take into account the velocity differences at various points in a cross-section of a stream, *Annales des Fonts et Chaussees*, 1, Ser. 1, 11, 314-335, 1836 (in French).

Cui, H., and Singh, V.P., Two dimensional velocity distribution in open channels using Tsallis entropy, *J. Hydrol. Eng.*, 18(3), 331–339, 2013.

Cui, H., and Singh, V.P., One dimensional velocity distribution in open channels using Tsallis entropy, *J. Hydrol. Eng.*, 19(2), 290–298, 2014.

Cover, T.M. and J.A. Thomas, *Elements of Information Theory*, NewYork: Wiley, 1991.

Despax A., C. Perret, R. Garçon, A. Hauet, A. Belleville, J. Le Coz, and A.C. Favre, Considering sampling strategy and cross-section complexity for estimating the uncertainty of discharge measurements using the velocity-area method, *Journal of Hydrology*, 533, 128-140, 2016.

Dingman, S. L., Probability distribution of velocity in natural channel cross-sections, *Water Resour. Res.*, 25(3), 509–518, 1989.

Dimitriadis, P., *Hurst-Kolmogorov dynamics in hydrometeorological processes and in the microscale of turbulence*, PhD thesis, Department of Water Resources and Environmental Engineering, National Technical University of Athens, 2017.

Dimitriadis, P., Three-dimensional simulation of flow at the location of the Atsicholos bridge on the river Loussios, Open Hydrosystem Information Network – OpenHI, HYDRONET (15), Vol. 4.1, 2018 (internal report in Greek).

Dimitriadis, P., and D. Koutsoyiannis, Stochastic synthesis approximating any process dependence and distribution, *Stochastic Environmental Research & Risk Assessment*, 32 (6), 1493–1515, doi:10.1007/s00477-018-1540-2, 2018.

Dimitriadis, P., D. Koutsoyiannis, and P. Papanicolaou, Stochastic similarities between the microscale of turbulence and hydrometeorological processes, *Hydrological Sciences Journal*, 61 (9), 1623–1640, doi:10.1080/02626667.2015.1085988, 2016a.

Dimitriadis, P., A. Tegos, A. Oikonomou, V. Pagana, A. Koukouvinos, N. Mamassis, D. Koutsoyiannis, and A. Efstratiadis, Comparative evaluation of 1D and quasi-2D hydraulic models based on benchmark and real-world applications for uncertainty assessment in flood mapping, *Journal of Hydrology*, 534, 478–492, 2016b.

Dimitriadis, P., A.D. Koussis, N. Kappos, D. Katsanos, S. Lykoudis, K. Mazi, and E. Rozos, Entropy-maximization method of discharge determination revisited: a stochastic-deterministic framework for estimating spatial velocity profiles in open-channel flow and its implications for sampling, *European Geoscience Union General Assembly*, EGU2019-15259, Vol. 21, 2019a.

Dimitriadis, P., A.D. Koussis, D. Koutsoyiannis, Estimating the hydraulic profiles of velocity, pressure and depth in natural cross-sections by employing the entropy maximization principle under one-dimensional steady-flow dynamics: II. Applications, 2019b (submitted).

Domeneghetti, A., Castellarin, A., and Brath, A.: Assessing rating-curve uncertainty and its effects on hydraulic model calibration,Hydrol. Earth Syst. Sci., 16, 1191–1202, doi:10.5194/hess-16-1191-2012, 2012.

Farina, G., S. Alvisi, M. Franchini, T. Moramarco, Three methods for estimating the entropy parameter M based on a decreasing number of velocity measurements in a river cross-section, *Entropy*, 16 (5), 5222512–2529, 2014.

Farina, G., Alvisi, S., Franchini, M., Corato, G., Moramarco, T., Estimation of bathymetry (and discharge) in natural river cross-sections by using an entropy approach, *J. Hydrol.*, 527, 20–29, 2015.

Fontana, N., G. Marini, and F. De Paola, Experimental assessment of a 2-D entropy-based model for velocity distribution in open channel flow, *Entropy*,15, 988–998, doi:10.3390/e15030988, 2013.

Fulton, J., and J. Ostrowski, Measuring real-time streamflow using emerging technologies: Radar, hydroacoustics, and the probability concept, *J. Hydrol.*,357(1), 1–10, 2008.

Gibbs, J.W., On the equilibrium of heterogeneous substances, *Trans Connect Acad. Sci.*, 16:343-524, 1878.

Greco, M., Effect of bed roughness on 1-D entropy velocity distribution in open channel flow, *Hydrol. Res.*, 46, 1–10, 2015.

Greco, M., Entropy-based approach for rating curve assessment in rough and smooth irrigation ditches, *J. Irrig. Drain Eng.*, 142, 04015062, 2016.

Greco, M., and Mirauda, D., Entropy parameter estimation in large-scale roughness open channel, *J. Hydrol. Eng.*, 20, 2015.

Greco, M., and Moramarco, T., Influence of bed roughness and cross-section geometry on medium and maximum velocity ratio in open-channel flow, *J. Hydraul. Eng.*,10, 2015.

Greco, M., Mirauda, D., Plantamura Volpe, A., Manning's roughness through the entropy parameter for steady open channel flows in low submergence, *Procedia Eng.*, 70, 773–780, 2014.

Guo, J., and Julien, Y.P., Shear stress in Smooth Rectangular Open Channel Flows, 131:1(30), 2005.

Hemelrijk, J., *Underlining random variables*, Statistica Neerlandica, 20 (1), 1966.

Jaynes, E.T., Information theory and statistical mechanics, *Phys. Rev.*, 106, 620–630, 1957.

Jiang, Y.; Bin, L.; Chen, J., Analysis of the Velocity Distribution in Partially-Filled Circular Pipe Employing the Principle of Maximum Entropy, PloS ONE, 11, 1-17, 2016.

Joseph, D.D., Potential flow of viscous fluids: historical notes, *Int. J. Multiphase Flow*, 32, 285–310, 2006.

Kazemian, K.K., H. Bonakdari, A. Gholami, Z.S. Khozani, A.A. Akhtari, and B. Gharabaghi, Uncertainty analysis of shear stress estimation in circular channels by Tsallis entropy, *Physica A: Statistical Mechanics and its Applications*, 510, 558-576, 2018.

Kazemian K.K.A., H. Bonakdaria, A. Gholamia and B. Gharabaghib, The uncertainty of the Shannon entropy model for shear stress distribution in circular channels, *International Journal of Sediment Research*, 2019.

Kàrman, T., Mechanische Ähnlichkeit und Turbulenz, Nachrichten von der Gesellschaft der Wissenschaften zu Göttingen, *Fachgruppe 1 (Mathematik)*, 5: 58–76, 1930.

Khozani, Z.S.; and Bonakdari, H., Formulating the shear stress distribution in circular open channels based on the Renyi entropy, *Physics A*, 490, 114–126, 2018.

Koussis, A., Ein Verbessertes Näherungsverfahren zur Berechnung von Hochwasserabläufen (An improved approximate flood routing method), Tech. Report no. 15, Institut für Hydraulik und Hydrologie, Technische Hochschule Darmstadt, Germany, 1975. [in German]

Koutsoyiannis, D., Uncertainty, entropy, scaling and hydrological stochastics, 1, Marginal distributional properties of hydrological processes and state scaling, *Hydrological Sciences Journal*, 50 (3), 381–404, doi:10.1623/hysj.50.3.381.65031, 2005.

Koutsoyiannis, D., HESS opinions A random walk on water, *Hydrology and Earth System Sciences*, 14, 585–601.doi:10.5194/hess-14-585-2010, 2010.

Koutsoyiannis, D., Hurst-Kolmogorov dynamics as a result of extremal entropy production, *Physica A: Statistical Mechanics and its Applications*, 390 (8), 1424–1432, 2011.

Koutsoyiannis, D., Entropy: from thermodynamics to hydrology, *Entropy*, 16 (3), 1287–1314, doi:10.3390/e16031287, 2014.

Koutsoyiannis, D., Stochastics of Hydroclimatic Extremes – A Cool Look at Risk, 2020 (in preparation).

Koutsoyiannis, D., P. Dimitriadis, F. Lombardo, and S. Stevens, From fractals to stochastics: Seeking theoretical consistency in analysis of geophysical data, *Advances in Nonlinear Geosciences*, edited by A.A. Tsonis, 237–278, doi:10.1007/978-3-319-58895-7_14, Springer, 2018.

Kumbhakar, M., K. Ghoshal, Two dimensional velocity distribution in open channels using Renyi entropy, *J. Physica A.*, 450, 546-559, 2016.

Kumbhakar, M., K. Ghoshal, and V.P. Singh, Derivation of Rouse equation for sediment concentration using Shannon entropy, *Physica A*, 465, 494–499, 2017a.

Kumbhakar, M., K. Ghoshal, and V.P. Singh, Renyi entropy and random walk hypothesis to study suspended sediment concentration, *J. Hydrol. Eng.*, 22(8), 04017027, 2017b.

Kumbhakar, M., S. Kundu, and K. Ghoshal, An explicit analytical expression for bed-load layer thickness based on maximum entropy principle, *Phys. Lett. A*, 382(34), 2297–2304, 2018.

Kumbhakar, M., K. Ghoshal, and V.P. Singh, Two-dimensional distribution of streamwise velocity in open channel flow using maximum entropy principle: incorporation of additional constraints based on conservation laws, 2019a (submitted).

Kumbhakar, M., K.R. Ray, S.K. Chakraborty, K. Ghoshal, and V.P. Singh, Mathematical Modelling of Streamwise Velocity Profile in Open Channels Using Tsallis Entropy, *Computational Physics*, arXiv:1910.12534, 2019b (submitted).

Kumbhakar, M., K.R. Ray, S.K. Chakraborty, K. Ghoshal, and V.P. Singh, On the Role of Tsallis Entropy Index for Velocity Modelling in Open Channels, *Computational Physics*, arXiv:1910.11665, 2019c (submitted).

Lighthill, M.J., and G.B. Whitham, On kinematic waves, I. Flood movement in long rivers, *Proc. R. Soc. London*, Set. 4, 229, 281-316, 1955.

Lollino, G., Arattano, M., Rinaldi, M., Giustolisi, O., Marechal, J.C., Grant, G.E., Eds.; Springer: Cham, Switzerland, Volume 3, pp. 641–645, ISBN 978-3-319-09054-2.

Maghrebi, M.F., and M. Rahimpour, A simple model for estimation of dimensionless isovel contours in open channels, *Flow Meas. Instrum.*, 16, 347–352, 2005.

Maghrebi M.F., and M. Rahimpour, Streamwise velocity distribution in irregular shaped channels having composite bed roughness, *J. Flow Meas Instrum.*, 17:237–245, 2006.

Manfreda, S., On the derivation of flow rating-curves in data-scarce environments, *J. Hydrol.*, 562, 151–154, 2018.

Marini, G., Martino, G. D., Fontana, N., Fiorentino, M., and Singh, V. P., Entropy approach for 2D velocity distribution in-open channel flow, *J. Hydraul. Res.*, 49(6), 784–790, 2011.

Marini, G., Fontana, N., and Singh, V.P., Derivation of 2D velocity distribution in watercourses using entropy, *Journal of Hydrologic Engineering*,22(6), 2017.

Mead L.R., and N. Papanicolaou, Maximum entropy in the problem of moments, *Journal of Mathematical* Physics, 25(8): 2404–2417, 1984.

Metropolis, N., *The beginning of the Monte Carlo method*, From cardinals to chaos, ed. by N.G. Cooper, Cambridge University, NY., 1989.

Mirauda, D., Pannone, M., and De Vincenzo, A., An entropic model for the assessment of stream-wise velocity dip in wide open channels, *Entropy*, 20, 69, 2018.

Moramarco, T., Saltalippi, C., and Singh, V. P., Estimating the cross-sectional mean velocity in natural channels using Chiu's velocity distribution, *J. Hydrol. Eng.*, 9(1), 42–50, 2004.

Moramarco, T.; Corato, G.; Melone, F.; Singh, V.P., An entropy-based method for determining the flow depth distribution in natural channels, *J. Hydrol.*, 497, 176–188, 2013.

Moramarco, T.; Barbetta, S.; Tarpanelli, A. From surface flow velocity measurements to discharge assessment by the entropy theory, *Water*, 9, 120, 2017.

Moramarco, T., S. Barbetta, D.M. Bjerklie, J.W. Fulton and A. Tarpanelli, River Bathymetry Estimate and Discharge Assessment from Remote Sensing, *Water Resources Research*, 2019.

Ohtsu, I., Y. Yasuda, and M. Takahashi, Flow Characteristics of Skimming Flows in Stepped Channels, *ASCE*, 130 (9), 2004.

Papadimitrakis, I.A., and Orphanos, I., Statistical analysis of river characteristics in Greece, basic hydraulic parameters, *Hydrological Sciences Journal*, Vol. 54, Issue 6, pp. 1035-1052, 2009.

Papoulis, A., Probability, Random Variables and Stochastic Processes, 3rd ed., *McGraw Hill*, NewYork, 1991.

Peppa, M.V., Application of geostatistical interpolation methods for estimating the mean velocity in a trapezoidal cross-section, MSc thesis, 91 pages, Athens, October 2008.

Pizarro, A., C. Samela, M. Fiorentino, O. Link, and S. Manfreda, BRISENT: An Entropy-Based Model for Bridge-Pier Scour Estimation under Complex Hydraulic Scenarios, *Water*, 9, 889, 2017.

Prandtl, L., *Verhandlungen des dritten internationalen Mathematiker-Kongresses in Heidelberg 1904*, edited by A. Krazer, Teubner, p. 484, Leipzig, Germany, [English translation in Early Developments of Modern Aerodynamics, edited by J. A. K. Ackroyd, B. P. Axcell, and A. L. Ruban, Butterworth- Heinemann, Oxford, UK, 2001], 1905.

Rahimpour M., Dimensionless isovelocity contours in rectangular cross-sections by harmonic mean distances, *Journal of Hydraulic Engineering*, 23 (3), pp. 241-245, 2017.

Rajaratnam, N., and D. Muralidhar, Boundary shear distribution in rectangular open channels, *La Houille Blanche*, 24(6), 603–609, 1969.

Rockinger, M., and E. Jondeau, Entropy densities with an application to autoregressive conditional skewness and kurtosis, *J. Econ.*, 106, 119 142, 2002.

Rudman, M., L.J.W. Graham, H.M. Blackburn, L. Pullum, Non-Newtonian turbulent and transitional pipe flow, in the 15th International Conference on Hydrotransport: incorporating the 11th International Symposium of Freight Pipelines, Banff (Canada), BHR Group Limited, the Fluid Engineering Centre, 2002.

Santana, D., Rodriguez-Rodriguez, J., Almedros-Ibanez, J.A., Martinez-Bazan, C., Characteristics lengths and maximum entropy estimation from probe signals in the ellipsoidal bubble regime, *International Journal of Multiphase Flow*, 32, 1123–1139, 2006.

Sasso, F.D., A. Pizarro, C. Samela, L. Mita, and S. Manfreda, Exploring the optimal experimental setup for surface flow velocity measurements using PTVS, *Environ. Monit. Assess.*, 190:460, 2018.

Schlichting, H., *Boundary Layer Theory*, McGraw-Hill, New York, 1960.

Schlichting, H., and K. Gersten, *Boundary-layer theory*, Graduate Texts in Mathematics, Springer-Verlag, 2017.

Sheikh, Z., and H. Bonakdari, Prediction of boundary shear stress in circular and trapezoidal channels with entropy concept, *Urban Water Journal*, 13(6), 629-636, 2015.

Shannon, C.E., A Mathematical Theory of Communication, *The Bell System Technical Journal*, Vol. 27, Oct., pp . 623-656, 1948.

Singh, V.P., Derivation of furrow geometry using entropy theory, *Trans. ASABE*, 55(3), 987–993, 2012.

Singh, V.P., *Entropy theory in hydraulic engineering: an introduction*, American Society of Civil Engineers, 2014.

Singh, V.P., and Luo, H., Entropy theory for distribution of one-dimensional velocity in open channels, *J. Hydrologic Eng.*, 10.1061/(ASCE)HE.1943-5584.0000363, 725–735, 2011.

Singh, V.P., Marini, G., and Fontana, N., Derivation of 2D power-law velocity distribution using entropy theory, *Entropy*, 15, 1221–1231, 2013.

Schmitt F.G., About Boussinesq's turbulent viscosity hypothesis: historical remarks and a direct evaluation of its validity, *Comptes. Rendus Mécanique*, 335: 617–627, 2007.

Temple, D.M., Velocity distribution coefficients for grass-lined channels, *J. Hydraul. Eng.*,112(3), 193–205, 1986.

Wibowo, H., Manning Roughness Coefficient Study on Bed Materials Non-Cohesive with Parameters Using Entropy to Open Channel Flow, *Proceedings of International Conference*: Issues, Management And Engineering In The Sustainable Development On Delta Areas Semarang, Indonesia – February 20th, 2015.

Yang, S.Q.; Tan, S.K.; Lim, S.Y., Velocity distribution and dip-phenomenon in smooth uniform channel flows, *J. Hydraul. Eng.*, 130, 1179–1186, 2004.

Yang, S.Q.; Tan, S.K.; Wang, X.K., Mechanism of secondary currents in open channel flows, *Geophys. Res.*, 117, F04014, 2012.

Yen, B. C., *Characteristics of subcritical flow in a meandering channel*, Tech. Report, Inst. of Hydr. Res., Univ. of Iowa, Iowa City, Iowa, 1965.

Yen, B.C., Open-channel flow equations revisited, *J. Eng. Mech. Div., Am. Soc. Civ. Eng.*,99(5), 979–1009, 1973.

Yoon, J.I., Sung, J., and Lee, M.H., Velocity profiles and friction coefficients in circular open channels, *Journal of Hydraulic Research*, 50:3, 304-311, doi:10.1080/00221686.2012.673745, 2012.

Zhu, Z. and Yu, J., Estimating the Bed-Load Layer Thickness in Open Channels by Tsallis Entropy, *Entropy*, 21, 123, 2019.